Journal of Combinatorial Mathematics and Combinatorial Computing
www.combinatorialpress.com/jcmcc

Combinatorial Press

A multi-objective linear programming model for optimizing the distribution of native vegetation suitability in Hanzhong, China

Jie Wu[1,✉], Haozhe Yu[1], Jing Zhang[2], Jiangtao Fu[3]

[1] *Department of Geographical Sciences, Shaanxi University of Technology, Hanzhong, Shaanxi 723001, China*

[2] *Innovation Team on Geo-Human Relationship and Sustainable Development in the Qinba Region, Shaanxi University of Technology, Hanzhong, Shaanxi, 723001, China*

[3] *Center for Geological and Environmental Research on Rock and Soil in the Qinba Mountains, Shaanxi University of Technology, Hanzhong, Shaanxi, 723001, China*

ABSTRACT
This paper takes the native vegetation in Hanzhong City as the research object, and constructs a multi-objective linear programming model to optimize the distribution of the suitability of the native vegetation in Hanzhong City. The ArcGIS software was used to test the sample consistency and screen the environmental variables of the native vegetation data in Hanzhong City represented by alfalfa, and the model in the software was used to predict the distribution of alfalfa's suitability area. Based on the prediction results, this paper constructs a multi-objective linear planning model with economic and ecological benefits as the objective function and the land area of different utilization types as the decision variables to optimize the distribution of the suitability of native vegetation in Hanzhong. At the same time, the fuzzy mathematical planning method was used to solve the constructed model. After the model optimization, the area of fitness distribution of native vegetation in Hanzhong City increased significantly, and the growth of the fitness distribution area of each vegetation by 2080 was 49.61%, 35.51%, 36.41%, 28.11%, 15.36%, 24.75%, 27.92%, 28.40%, 31.22%, and 31.52%, respectively. In addition, the optimization of the distribution of native vegetation suitability using the model of this paper can produce obvious economic and ecological benefits, which fully demonstrates the effectiveness of the model of this paper.

Keywords: multi-objective linear programming, fuzzy mathematical programming, objective function, decision variables, vegetation suitability

1. Introduction

Native vegetation refers to plants growing in or around the region, which are usually well adapted to the local environment and play important ecological and economic functions [1]. Drawing on the

✉ Corresponding author.
E-mail address: wujiesysu@126.com (J. Wu).

Received 05 March 2024; Revised 25 May 2024; Accepted 05 December 2024; Published Online 15 April 2025.
DOI: 10.61091/jcmcc127a-241

existing vegetation classification system, native vegetation can be broadly categorized into world geographic native vegetation and regional native vegetation according to the differences in geographic location, and Hanzhong native vegetation belongs to the latter [2].

Hanzhong City is located in the southwestern part of Shaanxi Province, which is situated in the transition zone of the warm-temperate zone, with four distinct seasons, hot and rainy summers, and dry and cold winters. Hanzhong City has a wide range of vegetation cover, including forests, grasslands, wetlands, etc. It is characterized by a wide variety of species, complex composition of zones, diverse vegetation types, and obvious vertical structure [3-4]. The plant species and vegetation types are different in different natural areas. For example, the Han River valley has deciduous broad-leaved forests mixed with evergreen broad-leaved species reflecting subtropical climate [5]. Whereas, the Qinba Mountains have deciduous broad-leaved forests, mixed coniferous and broad-leaved forests and coniferous forests reflecting the warm-temperate and mesotemperate climatic environments [6]. In addition, native vegetation has the basic characteristics of regionality, adaptability, resilience, economy, inner richness, and penetration and expansion due to its geographical distinction [7-10]. Its adaptability is due to the diversity of climatic and geographic conditions, native vegetation needs to be adapted to different environmental stresses in order to survive [11-13]. For example, some plants are adapted to cold climatic conditions, such as rhododendrons and tundra plants in the high mountains, while some are adapted to arid environments, such as desert plants and steppe plants in the north. Native vegetation is also adapted to different soil types, such as acidic, alkaline and infertile soils [14]. This wide range of adaptability enables native vegetation to survive and reproduce under a variety of environmental conditions, and plays an important role in the restoration and protection of the ecological environment.

The native vegetation of a region is closely related to the local environment, and human activities, soil nourishment, water purification, agricultural cultivation, as well as the adsorption of airborne dust and the transformation of harmful gases are all indispensable factors for the stabilization of the ecological structure of the region [15-18]. The loss of native vegetation not only affects the biodiversity and microclimate of the region, but also jeopardizes the stability of the whole ecosystem.

In this paper, the geographic location, topography and soil vegetation of Hanzhong City were introduced in detail, and alfalfa was used as the representative of native vegetation in Hanzhong City to select sample sites. With the help of ArcGIS technology, the consistency test of the selected sample data was carried out, and the environmental variables were screened by the significance analysis of the correlation coefficient matrix between each environmental variable. The model in ArcGIS software was utilized to predict the changes in the adaptive distribution area of the native vegetation in Hanzhong City represented by alfalfa in the time periods of 2030, 2050 and 2080. Cultivated land area, vegetation area, construction land area, water area and unutilized land area were selected as decision variables in the process of optimizing the distribution of native vegetation in Hanzhong City, and a multi-objective linear programming model was constructed to optimize the distribution of native vegetation in Hanzhong City by setting a series of constraints without the objective function of economic and ecological benefits. The performance of the model is demonstrated by comparing the changes in the area of native vegetation habitability distribution before and after the optimization, and the benefits achieved by different models in optimizing the distribution of native vegetation habitability.

2. Overview of the study area

2.1. Geographical location

Hanzhong City is located in southwestern China and southwestern Shaanxi Province, and its geographic location is shown in Figure 1. It is neighboring with Baoji and Xi'an City of Shaanxi Province in the north, bordering with Ankang City of Shaanxi Province in the east, linking with Longnan City of

Gansu Province in the west, and bordering with Guangyuan City and Bazhong City of Sichuan Province in the south. Geographic location 105°30′ 50″ -108°16′ 45″ E, 32°08′ 54″ -33°53′ 16″ N. East-west length of 258.6km, north-south width of 192.9km, covering an area of 27246km^2, accounting for 13.24% of the total area of the province.

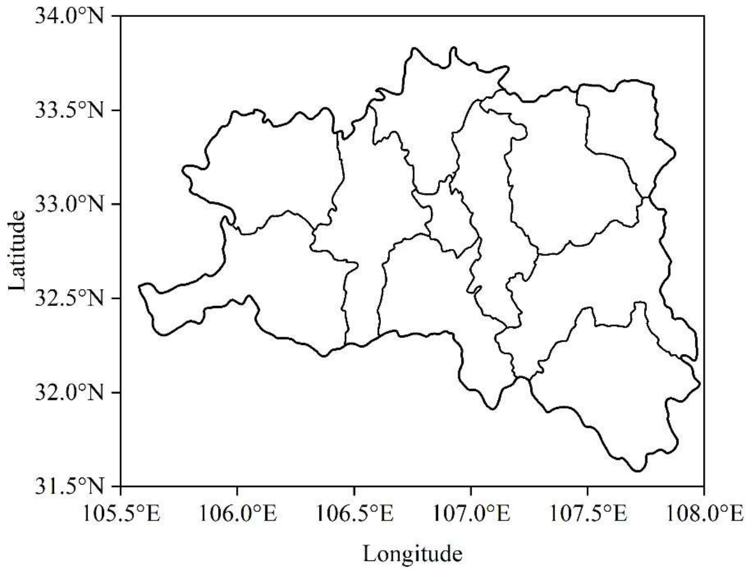

Fig. 1. Geographic location

2.2. *Topography and geomorphology*

Hanzhong City has a large mountainous area, "eight mountains, one water, one field", with complex and varied topography and geomorphology. The terrain is high in the north and south and low in the middle, from north to south, it is the Qinling Mountain area, Han River Valley area and Bashan Mountain area. The Han River runs across the basin from west to east, becoming the natural boundary between the two mountain systems. The Qinling Mountains stretch from east to west, with an average elevation of about 2000 meters. The mountains are undulating, with many rivers and faults developing, and the broken line basin is interspersed with river valleys and river valleys, and the rocks are broken, and the weathered layer is deep and loose. There are three landform types in the Qinling Mountain area, namely Zhongshan Mountain, Low Mountain and Hills, with less distribution of hilly landforms, just along the northern edge of the Hanzhong Basin, with an elevation of about 600 m. Zhongshan Mountain is mainly distributed along the south bank of the Muma River, Ningqiang and Lianshui River Basin and Jialing River Basin, with an elevation of mostly 1,000 to 1,200 m, with slow slopes, thick soil layers and better soil development. The Bashan Mountain Range runs east to west and is slightly lower than the Qinling Mountain Range, with no peaks exceeding 3,000 meters, but it is very steep, with an average elevation of about 2,000 meters. The mountainous area of Hanzhong accounts for about 75.2% of the total land area, the hills account for 14.6%, and the flat dams account for 10.2%. The elevation of Hanzhong Basin is about 500m above sea level, and the Qinba Mountains are about 500~2500m above the Hanzhong Basin.

2.3. *Soil vegetation*

Hanzhong City has large differences in topography and geomorphology, and the soil formation process is complicated, so the soil types are diverse. Hanzhong city soil belongs to the soil of the region, in the country belongs to the aluminum soil domain yellow-brown soil belt, there are 10 soil classes, 21 subclasses, 38 soil genera, 97 soil species. Agricultural soil is mainly yellow-brown soil. The yellow-brown soil is the main zonal soil in Hanzhong City, which is distributed in the hills and valleys below

1500m on the south slope of Qinling Mountain and below 1800m on the north slope of Ba Mountain. The mountain brown soil in Hanzhong City is distributed in the middle mountain forest belt above 1500~2200m on the south slope of Qinling Mountain and 1800~2000m on the north slope of Bashan Mountain, which is an important forest soil. It is rich in forest products and has favorable conditions for forestry development. Rice soil is the main cultivation soil in Hanzhong area, mainly distributed in the first and second terraces along Jianghan and its tributaries, as well as Hantai and Xixiang basins. Lime soil is mainly distributed in Zhenba, Ningqiang, Xixiang, Nanzheng and Luoyang, Liuba, Mianxian and other places.

The vegetation in Hanzhong City is varied and complex, with obvious vertical structure. The Han River valley has a deciduous broad-leaved forest belt mixed with evergreen broad-leaved species, and the Qinba Mountain area is mainly deciduous broad-leaved forests, coniferous forests and mixed coniferous and broad-leaved forests. The vegetation of Han River basin consists of secondary plantation forests, shrub forests and grasslands, and among the existing secondary forests, the proportion of tree forests, which are mainly used for timber and protection, is larger, reaching about 70%. Tree species mainly include oil pine, cypress, sequoia, etc., economic forests mainly include ginkgo, tea, walnut, citrus, etc., and grasses mainly include lobelia, alfalfa and other weeds.

3. Data sources and processing

There are many types of vegetation in Hanzhong City, which would cause great trouble for the study if analyzed one by one. Therefore, in order to simplify the analysis, this paper chooses to use alfalfa as a representative of vegetation to analyze the distribution of native vegetation suitability in Hanzhong.

3.1. Sample data

3.1.1. Sample data sources. The distribution data of alfalfa in Hanzhong City were mainly obtained by reviewing and organizing the relevant websites of various countries, the platform of standardized organization, integration and resource sharing of teaching specimens, the relevant literature of various countries, and the experimental data of field investigation. By combining the above ways, a total of 724 sample points of alfalfa distribution were obtained in this paper.

3.1.2. Sample data screening. Since the accuracy of the locus distribution data directly affects the simulation and prediction results of the model, this experiment obtained the current vegetation type map of the study area according to the analysis of land cover types of the International Geosphere Biosphere Program with the help of Arc GIS technology, and eliminated the locus distribution data of the alfalfa vegetation part, and finally obtained the accurate distribution data of 315 loci as shown in Figure 2.

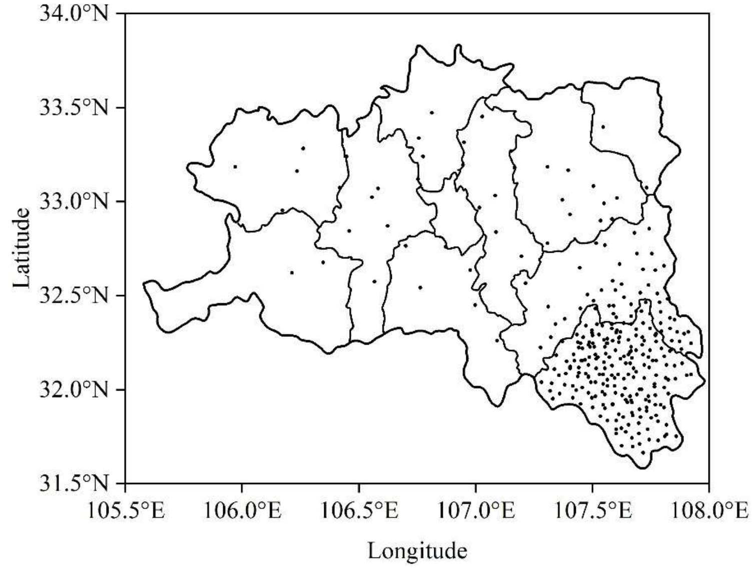

Fig. 2. Sample point distribution

3.1.3. Sample set consistency test. The total sample set containing 315 loci distribution data was divided into samples in the ratio of 3:1, and the number of loci in the training sample set was obtained to be 210, and the number of loci in the test sample set was 105. The attribute values of the sample points corresponding to the environmental variables were extracted using ArcGIS, and the Kolmogorov-Smirnov test [19] was performed on the two sample sets. The K-S test determines whether the observations of the samples are from the same distribution of the total by analyzing the differences between the two distributions. The results show that the p-values of the K-S test are all greater than 0.1, so the original hypothesis is accepted and the two sample sets are considered to be from the same distribution of the whole.

3.2. Environmental variable data

3.2.1. Environmental data preparation. The environmental variable data include two major parts of data, the current dataset (1988-2023) and the future dataset (2030s-2080s), each dataset includes 72 environmental variables each, and some of the variables are shown in Table 1. Among them, the topographic variable data mainly include elevation, slope and slope direction, the elevation data are derived from SRTM data, the SRTM topographic data used are SRTM3 with a resolution accuracy of 100M data, while the slope and slope direction factors are calculated from the elevation data. Climate variable data include air temperature, precipitation, humidity (K), $\geq 0^{\circ}C$ -year cumulative temperature ($\sum\theta$) and 17 bioclimatic factors (Bio1-17), etc. The air temperature, precipitation and bioclimatic factors were obtained from the WorldClim environmental database, whereas the humidity and $\geq 0^{\circ}C$ -year cumulative temperature data were computed and calculated according to the humidity model, in which r is the annual precipitation (mm) and $\sum\theta$ is the $\geq 0^{\circ}C$ -year cumulative temperature. The spatial resolution of the environmental data is 35s.

Table 1. Partial environment variable

Environmental variable	Meaning	Environmental variable	Meaning
Alt	Altitude	Bio 8	Average temperature of the wet quarter
Aspect	Slope aspect	Bio 9	Average temperature of the most dry quarter
Slope	Slope	Bio 10	Average temperature of the warmest quarter
Prec 1-12	Precipitation from 1 to 12	Bio 11	Average temperature of the coldest quarter
Tmax 1-12	Maximum temperature from 1 to 12	Bio 12	Annual average precipitation
Tmenan 1-12	Mean temperature from 1 to 12	Bio 13	Precipitation variation coefficient
Tmin 1-12	Minimum temperature from 1 to 12	Bio 14	Wet quarter precipitation
Bio 1	Annual average temperature	Bio 15	Most dry quarter precipitation
Bio 2	Monthly average temperature difference between day and night	Bio 16	Warmest quarter precipitation
Bio 3	The ratio of diurnal temperature difference to annual temperature difference	Bio 17	Coldest quarter precipitation
Bio 4	Standard deviation of seasonal temperature variation	K	Wetness
Bio 5	Maximum temperature of the most warm month	$\sum\theta$	$\geq 0^{\circ}C$ annual accumulation temperature
Bio 6	Minimum temperature of the coldest month	Sand 2	Bottom sand content
Bio 7	The range of changes in average annual temperature	Clay 2	Underlying clay content

Since the WorldClim database lacks data from 1989 onwards, this experiment was supplemented with data from 1988-2023, which were mainly obtained according to the methods provided on the WorldClim website using Anusplin, ArcGIS, and R. Anusplin is a tool that provides practical transformational analyses and interpolations of multivariate data using thin disk Smooth Spline Interpolation for interpolation. It provides all the statistical analysis, spatial distribution standard errors, and data diagnosis, and can also support a variety of data input and surface query functions. The station data for meteorological interpolation were mainly obtained from the China Meteorological Science Data Sharing Service Network (CMSDSN), and the temperature and precipitation data from 1988 to 2023 were fitted by thin-disk smooth spline interpolation with latitude and longitude as the independent spline variables and elevation as the covariate through the Anusplin software, using the longitude and latitude as the independent spline variables and elevation as the covariate. 17 bioclimatic factors were obtained by using “dismo” function packages of the R software. The 17 bioclimatic factors can be calculated using the “dismo” function package of the R software. The 17 bioclimatic factors can be calculated using the “dismo” function package in R. Similarly, the data for factors K and $\sum\theta$ were calculated by interpolating the results of temperature and precipitation.

3.2.2. Environmental data analysis and screening. Because all environmental variables are correlated with each other, which will affect the results of the model's screening of the importance of the factors, this study utilizes Arc GIS software to perform correlation analysis between 72 environmental variables, and uses the band collection statistics tool in ArcGIS to obtain the correlation coefficient matrix between each environmental variable for significance analysis. Finally, the environmental variables that were significantly correlated with other environmental variables were eliminated. At the same time, the MaxEnt model was run to screen the importance of environmental factors, analyze and determine the limiting environmental variables affecting the alfalfa suitability distribution model simulation, and screen out the environmental variables with higher contribution rate to the model simulation.

The set of environmental variables mainly included 72 variables such as elevation, slope, slope direction, temperature, precipitation, and bioclimatic factors. The 72 variables were correlated to obtain the correlation coefficient matrix and analyzed for significance, and seven environmental variables with highly significant correlations, such as slope direction, wetness value K, and bottom sand content, were finally excluded.

After eliminating the seven significantly correlated environmental variables, 65 environmental variables were finally identified for model pre-selection. In this study, in order to make the model simulation results more accurate, the current habitat distribution of alfalfa was repeatedly simulated, and according to the contribution rate of the variables in the model running results, the environmental variables with a contribution rate of 0 were excluded from the model simulation, and 32 environmental variables with a contribution rate of more than 0 were finally screened out as the environmental variables used in this study, and the results of the screening of environmental variables are shown in Table 2. From the contribution rate of environmental variables to the model, it can be seen that all 32 environmental variables have a certain contribution rate to the model simulated by the current distribution status of alfalfa, among which, the contribution rate of elevation is the most prominent, which reaches 39.48%, followed by the coefficient of variation of precipitation and the precipitation in December, which reaches 24.13% and 15.32%, respectively.

Table 2. The contribution rate of environment variable to model

Variable	Contribution/%	Variable	Contribution/%
Alt	39.48	Tmean 11	0.32
Bio 15	24.13	Prec 7	0.29
Prec 12	15.32	Bio 16	0.22
Bio 2	3.83	Tmean 3	0.18
Tmin 6	3.31	Tmean 8	0.13
Bio 13	2.76	Tmax 12	0.1
Clay 2	1.88	Prec 8	0.09
Prec 4	1.57	Tmean 6	0.09
Prec 1	1.13	Tmin 3	0.09
Bio 12	0.94	Tmax 7	0.09
Tmin 4	0.87	Bio 14	0.07
Prec 6	0.73	Tmax 11	0.06
Tmax 9	0.62	Prec 10	0.03
Tmin 5	0.58	Tmean 2	0.01
Bio 7	0.53	Tmean 10	0.01
Slope	0.47	Bio 9	0.01

4. Predicting the distribution of native vegetation suitability

4.1. Accuracy of simulation results

At this stage, the evaluation of simulation accuracy is usually done with the help of AUC value. It is the value of the area under the ROC curve, and the range of values is 0.5~1.0. It is generally considered that: when it is 0.5~0.60, it is set as failure; when it is 0.60~0.70, it is considered as poor; when it is 0.70~0.80, it is set as average; when it is 0.80~0.90, it is set as good; and when it reaches 0.90~1.00, it is recognized as excellent. The constructed model is considered usable when AUC>0.75, and the larger the AUC value, the better the prediction accuracy of the constructed model.

In this paper, Arc GIS software was utilized to predict the distribution of the suitability of Hanzhong native vegetation represented by alfalfa in Hanzhong. The prediction accuracy of the prediction model in the software was measured using the AUC value, and the results are shown in Figure 3. The AUC values of the model simulation and test results in the study reached 0.947 and 0.924, respectively, and the prediction accuracy reached an excellent level.

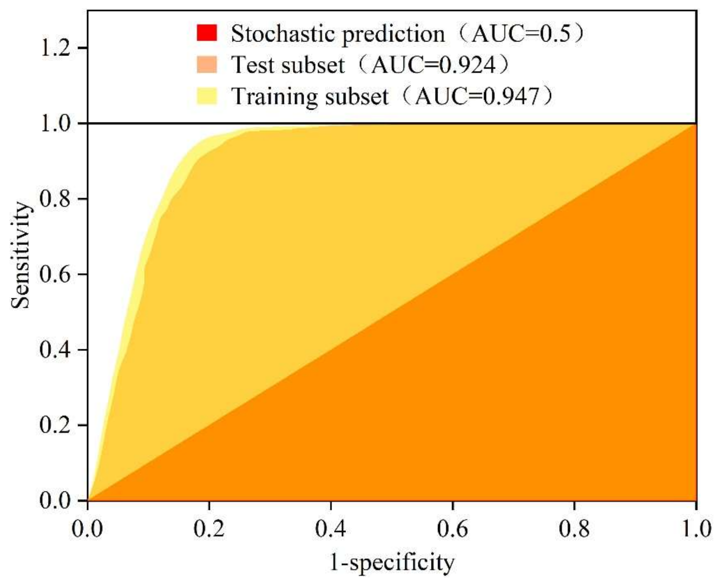

Fig. 3. Model prediction accuracy

4.2. Prediction of fitness distribution

Fig. 4 shows the prediction results of native vegetation suitability in Hanzhong represented by alfalfa, (a) is the "current" suitable distribution area in 2023, (b)-(d) is the distribution of alfalfa suitable area in 2030, 2050 and 2080, respectively, and H, M and L represent high suitability, moderate fertility and low fertility suitability, respectively. From the figure, it can be seen that the distribution of alfalfa suitable area shows a northward trend in general, and the area of suitable area shows a decreasing trend.In 2023, the alfalfa suitable area is mainly distributed in the south and southeast of Hanzhong. In 2023, the suitable area of alfalfa was mainly distributed in south Hanzhong and southeast Hanzhong, in which the moderate suitable area in the south was densely distributed in the form of strips, and the suitable area in southeast Hanzhong was densely distributed in the form of blocks, and it was mainly the dense distribution area of alfalfa that was highly suitable. Sparse distribution of alfalfa aptitude area also exists in most of the rest of Hanzhong. By 2030, with the change of climate conditions such as temperature and precipitation as well as other related factors, the suitable area of alfalfa will be changed, which is mainly manifested as: the original southern and southeastern suitable area will be shifted to the north, and the southern area will be changed from a medium suitable area to a highly suitable area. In 2050, the density of alfalfa habitat distribution decreased, leaving only the northeast as a highly suitable area for alfalfa. The original southern suitable area is no longer suitable for alfalfa, and the southeastern suitable area is shifted further north, and the degree of suitability is reduced to a low suitable area. The northwestern area has new dense areas of moderate suitability for alfalfa growth, but the area is small. By 2080, the alfalfa suitability area in Hanzhong is mainly densely distributed in the northwest, north and northeast areas, and there is no highly suitable area for alfalfa, and the area and degree of suitability and denseness of the area are decreasing sharply. It is expected that the suitable area of native vegetation represented by alfalfa in Hanzhong will face the possibility of disappearing in the future, and it is urgent to optimize the distribution area of vegetation suitability.

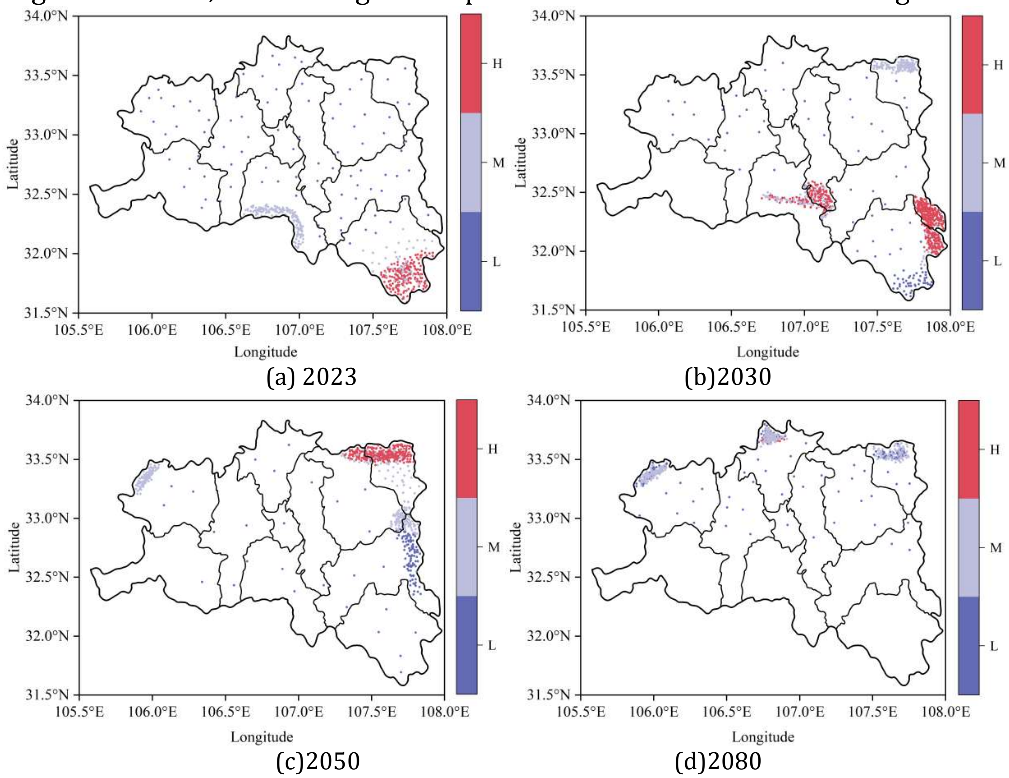

Fig. 4. Prediction of the distribution of alfalfa suitable areas

5. Multi-objective linear programming models to optimize fitness distribution

Multi-objective planning model, also known as multi-objective decision-making [20], is based on multi-objective decision-making theory to solve decision-making problems in resource management in the case of multiple conflicting and competing objectives, with multi-objective, multi-program features, which can make full use of the existing resources, and decision-makers to provide technical support for the development of relevant decisions. The advantage of multi-objective planning is that decision makers can formulate a variety of programs for their reference according to different criteria, and ultimately choose the most satisfactory configuration, so as to improve the scientific nature of the optimal allocation. The multi-objective linear programming model has two or more objective functions, and the objective functions and constraints are linear. In this study, a multi-objective linear programming model was used to establish an optimal allocation model for the distribution of the suitability of native vegetation in Hanzhong.

5.1. Modeling

5.1.1. Decision-making variables. There are many factors affecting the distribution of native vegetation suitability in Hanzhong, and the factors are interdependent and responsive to each other, and different influencing factors will produce different benefits, so the optimal allocation of the distribution of native vegetation suitability is a very complicated systematic project. The utilization of land resources determines the amount of demand for native vegetation resources, so in this study, we chose the land area of five utilization types, i.e., cropland area, vegetation area, construction land area, water area, and unutilized land area of seven districts and counties in Hanzhong City as the decision variables in the process of the optimization of the distribution of the suitability of native vegetation in Hanzhong City, and the results are shown in Table 3, with the C1-C7 in the table representing the 7 districts and counties.

Table 3. Decision variables

X_i^k	C1	C2	C3	C4	C5	C6	C7
Ploughing	X_1^1	X_1^2	X_1^3	X_1^4	X_1^5	X_1^6	X_1^7
Grass	X_2^1	X_2^2	X_2^3	X_2^4	X_2^5	X_2^6	X_2^7
Construction land	X_3^1	X_3^2	X_3^3	X_3^4	X_3^5	X_3^6	X_3^7
Waters	X_4^1	X_4^2	X_4^3	X_4^4	X_4^5	X_4^6	X_4^7
Unexploited land	X_5^1	X_5^2	X_5^3	X_5^4	X_5^5	X_5^6	X_5^7

5.1.2. Objective function. The objective functions established in this study are as follows:
1) Economic efficiency objective. The most intuitive reflection of economic efficiency is the gross national product of the region. This study adopts the maximum GNP generated by different types of land as the economic efficiency objective, i.e.:

$$\max F_i(X) = \sum_{k=1}^{7}\sum_{i=1}^{5} a_i^k X_i^k \tag{1}$$

Where: i denotes land type; a_i^k denotes GDP generated per unit area of k region (county) i type of land (million yuan/ km^2). X_i^k is the area of the k region i type of land (km^2).

The coefficient a_i^k is the ratio of the total GDP of each type of land in each district and county to the corresponding total area of each type of land, calculated as shown in Table 4.

Table 4. Calculation result of a_i^k

a_i^k	C1	C2	C3	C4	C5	C6	C7
i_1	198.43	132.56	84.73	189.64	489.38	127.64	290.57
i_2	732.04	113.59	52.74	268.31	83.78	42.16	122.93
i_3	13862.07	6849.56	9038.71	11253.44	23496.82	11992.47	41235.84
i_4	709.27	126.84	108.32	593.47	361.28	73.58	226.34
i_5	0	0	0	0	0	0	0

2) Eco-efficiency target. Eco-efficiency adopts the objective of minimizing the total amount of groundwater supply. Due to the shortage of surface water resources in the study area, the main source of water supply is groundwater, resulting in a high degree of groundwater exploitation and utilization and serious over-exploitation. Therefore, under the circumstance of meeting the water supply, the exploitation and utilization of groundwater resources should be as little as possible. Namely:

$$\min F_2(X) = \sum_{k=1}^{7}\sum_{i=1}^{5} b_i^k X_i^k \tag{2}$$

Where: b_i^k is the amount of water supplied from groundwater sources in the k counties to the i types of land per unit area (million $\mathrm{m}^3/\mathrm{km}^2$), and the other letters have the same meaning as above.

The coefficient b_i^k is the ratio of the amount of water that can be supplied by the groundwater supply project in each district and county to the total area of each land type, and the results of the calculation are shown in Table 5.

Table 5. Calculation result of b_i^k

b_i^k	C1	C2	C3	C4	C5	C6	C7
i_1	13.46	9.82	7.36	13.83	7.42	15.94	17.43
i_2	4.08	0.43	0.52	1.87	0.28	0.62	1.49
i_3	68.43	43.24	32.84	19.45	132.71	40.83	138.42
i_4	8.36	0.51	9.48	4.96	43.58	35.81	0
i_5	0	0	0	0	0	0	0

5.1.3. Constraints:

1) Water Resource Constraints. Water resource constraint, i.e., total water constraint, means that the sum of water demand of all types of land in each district and county should not exceed the amount of water resources available, i.e.,:

$$\sum_{k=1}^{1}\sum_{i=1}^{s} c_i X_i^k \le W \tag{3}$$

Where: c_i is the water use quota for each type of land. W is the amount of water resources available, using the average value of water supply from 1988 to 2023, while referring to the development plan of Hanzhong City and the restrictions on the development of groundwater to determine the amount of water resources available, i.e., W = 304,863,000 m^3, of which the amount of groundwater developed and utilized shall not exceed 2,786,340,000 m^3.

2) Total land area constraint. The total land area constraint means that the sum of each type of land is equal to the total amount of land resources. That is:

$$\sum_{k=1}^{7}\sum_{i=1}^{s} X_i^k = T \tag{4}$$

Where: T is the total area of each type of land, $T = 39483\mathrm{km}^2$.

The constraint areas of arable land and grassland are clearly defined in the 2000-2030 land use master plan of Hanzhong City.

Therefore, the constraints on the area of these two types of land can be determined as follows:

3) Cultivated land area constraint

$$10212.56 \le \sum_{k=1}^{7} X_1^k \le 16487.42 \tag{5}$$

4) Vegetation area constraints

$$16312.74 \le \sum_{k=1}^{7} X_2^k \le 23687.13 \tag{6}$$

5) Construction land constraints. With the development of industrialization and urbanization, there will be a certain degree of population growth, and the land for construction will inevitably grow with it, and therefore will be larger than the current area. Therefore:

$$\sum_{k=1}^{1} X_3^k \ge 627.44 \tag{7}$$

6) Restriction of water area. According to the current area of the rivers and ditches in Hanzhong City and the land area of the completed reservoir, then it can be stipulated that the watershed area shall not be smaller than the current area. That is:

$$\sum_{k=1}^{7} X_4^k \geq 148.22 \tag{8}$$

7) Unutilized land constraint. Unutilized land is dominated by sandy, saline and bare land, whose treatment and development is difficult to achieve in a short period of time, so the area of unutilized land is assumed to be constant. Namely:

$$\sum_{k=1}^{7} X_5^k = 4328.61 \tag{9}$$

8) Non-negative constraints on variables. Each variable should be greater than or equal to zero to ensure the validity of each variable. Namely:

$$X_1^k \geq 0 \tag{10}$$

5.2. Model solving

Multi-objective linear programming is an important part of multi-objective optimization theory, because each objective must be contradictory to each other, so it is impossible to make all the objectives at the same time to achieve the optimal solution, but only to find its effective solution (non-inferior solution). In this study, the fuzzy mathematical planning method is used to transform the multi-objective problem into a single objective [21], and the mathematical software Matlab is used to solve the optimal solution that satisfies the objective function and constraints at the same time.

The objective function and constraints of multi-objective linear programming are linear, and its mathematical model expression is:

Objective function:

$$\max Z = Cx \tag{11}$$

Constraints:

$$\begin{cases} Ax \leq b \\ x \geq 0 \end{cases} \tag{12}$$

Among them:

$$\begin{aligned} &Z = (Z_1, Z_2, \cdots, Z_1)^T \\ &A = (a_y)_{m \times n}; C = (C_{ij})_{r \times n} \\ &b = (b_1, b_2, \cdots, b_m)^T \\ &x = (x_1, x_2, \cdots, x_n)^T \end{aligned} \tag{13}$$

Since there is more than one objective function, to find a certain point as x^* so that the objective function can be satisfied, usually such an optimal solution does not exist. Therefore, the fuzzy mathematical planning method is used to defuzzify each objective function, transforming the complex multi-objective problem into a simple single-objective problem, so as to simplify the solution process and find the fuzzy optimal solution. The specific practices are as follows:

5.2.1. Solving the feasible region. First find the maximum value Z of each single objective $Z_i, i = 1, 2, \cdots, r$ under constraint $\begin{cases} Ax \leq b \\ x \geq 0 \end{cases}$:

$$Z_i^* = \max\left\{ Z_1 \mid Z_i \mid = \sum_{j=1}^{n} c_{ij}, Ax \le b, x \ge 0 \right\} \quad i = 1, 2, \cdots, r \tag{14}$$

For each objective function $Z, i = 1, 2, \cdots, r$, the corresponding fuzzy scaling factor $d_i (d_i > 0)$ is given, and the selection of scaling factor d_i should be chosen according to the importance of each sub-objective, and should follow the principle of "the more important the index scaling indicator is smaller", and fuzzy processing will be carried out for each sub-objective.

In this study, the value of the scaling factor d_i is taken as calculated in accordance with Eq. $d_i = Z_i^* - Z_i^-$. However, in the multi-objective planning problem, it is difficult for each sub-objective to reach the maximum value Z_i^* at the same time, but the range of its value can be determined, i.e., $Z_i^- \le Z_i \le Z_i^*$, where $Z_i^- = \min Z_i$.

For objective Z_i, a fuzzy objective $\tilde{M}_i$ is constructed and its affiliation function is defined as:

$$M_i = g_i\left(\sum_{j=1}^{n} c_{ij} x_j\right) \begin{cases} 0 & \sum_{j=1}^{n} c_{ij} x_j < Z_i^* - d_i \\ 1 - \dfrac{1}{d_i}\left(Z_i^* - \sum_{j=1}^{n} c_{ij} x_j\right) & Z_i^* - d_i \le \sum_{j=1}^{n} c_{ij} x_j \le Z_i^* \\ 1 & Z_i^* < \sum_{j=1}^{n} c_{ij} x_j \end{cases} \tag{15}$$

Remember:

$$\tilde{M} = \bigcap_{i=1}^{r} \tilde{M}_i \tag{16}$$

Then $\tilde{M}$ is said to be the fuzzy objective of the multi-objective linear programming problem, denoted:

$$D = \{ x \mid Ax \le b, x \ge 0 \} \tag{17}$$

Then D is the set of possible solutions satisfying the constraints, called the feasible solution domain.

5.2.2. Optimal solution using fuzzy judgments. Constructing fuzzy judgments as:

$$\tilde{D}_f = D \bigcap \tilde{M} \tag{18}$$

Is the optimal solution of $\tilde{M}(x)$ over the feasible solution domain D.

Then x^* satisfying $\tilde{D}_f(x^\bullet) = \max_{x \ge 0}(D(x) \wedge \tilde{M}(x)) = \max_{x \in D} \tilde{M}(x)$ is said to be the fuzzy optimal solution, i.e., x^* then the multi-objective problem is transformed into a single-objective problem, so as to find the optimal multi-objective solution. The transformation process is as follows: let: $\lambda = \tilde{M}(x) = \bigcap_{i=1}^{r} \tilde{M}_i$, then the fuzzy optimal solution to solve the multi-objective linear programming problem can be transformed into:

$$\begin{cases} \max Z = \lambda \\ \sum_{j=1}^{n} c_{ij} x_j - d_i \lambda \ge Z_i^* - d_i & i = 1, 2, \cdots, r \\ \sum_{j=1}^{n} a_{kj} x_j \le b_k & k = 1, 2, \cdots, m \\ \lambda \ge 0 & x_1, x_2, \cdots, x_n \ge 0 \end{cases} \tag{19}$$

The optimal solution $(x_1^*, x_2^*, \cdots, x_n^*, \lambda^*)$ .is calculated by MATLAB software, where $x^* = (x_1^*, x_2^*, \cdots, x_n^*)$ is the fuzzy optimal solution of multi-objective current planning.

5.3. Results and analysis

5.3.1. Optimization of the area distribution of the suitability of native vegetation. The multi-objective linear programming model was used to optimize the distribution of the suitability of the native vegetation in Hanzhong City, and the current and predicted changes in the suitability distribution area of the native vegetation represented by alfalfa before and after the optimization were obtained as shown in Table 6, in which V1-V10 denoted the 10 types of native vegetation in Hanzhong including alfalfa, and 2023 denoted the current status quo of the vegetation's suitability distribution area, and 2030, 2030, 2050 and 2080 represent the predicted vegetation habitability distribution area, respectively. From the table, it can be seen that the area of suitable distribution of each native vegetation increased significantly after optimization. At the current stage in 2023, for example, the area of suitability distribution of the 10 planted vegetation is 281.64 km^2, 224.07 km^2, 252.78 km^2, 236.42 km^2, 284.39 km^2, 245.03 km^2, 201.31 km^2, 267.25 km^2, 254.19 km^2, 237.72 km^2, compared to the pre-optimization growth of 9.01%, 66.56%, 59.41%, 94.42%, 6.82%, 69.70%, 13.70%, 6.72%, 43.30%, and 110.67%, respectively. In the projection of 2080, only 65.89 km^2, 71.05 km^2, 66.68 km^2, 69.23 km^2, 76.69 km^2, 73.94 km^2, 66.83 km^2, 69.65 km^2, 75.11 km^2, and 68.62 km^2 of the un-optimized vegetation distributions were left, respectively, and it is expected that they may decrease further in the future. And after optimization, the fitness distribution area of each vegetation increased by 49.61%, 35.51%, 36.41%, 28.11%, 15.36%, 24.75%, 27.92%, 28.40%, 31.22%, 31.52%, respectively. It shows that the multi-objective linear planning model constructed in this paper can effectively realize the growth of the area of the distribution area of the suitability of native vegetation in Hanzhong, so as to provide scientific support for the protection and restoration strategy of native vegetation in Hanzhong.

Table 6. Areal product change(km^2)

Vegetation	Before optimization				After optimization			
	2023	2030	2050	2080	2023	2030	2050	2080
V1	258.36	112.66	82.63	65.98	281.64	186.12	110.36	98.71
V2	134.53	91.53	83.5	71.05	224.07	166.92	103.08	96.28
V3	158.57	97.1	95.31	66.68	252.78	170.41	110.1	90.98
V4	121.6	103.12	81.78	69.23	236.42	162.83	104.66	88.69
V5	266.23	107.73	98.49	76.69	284.39	190.56	112.99	88.47
V6	144.39	99.85	93.19	73.94	245.03	186.22	116.37	92.24
V7	177.06	100.13	96.55	66.83	201.31	172.62	107.35	85.49
V8	250.42	103.45	95.89	69.65	267.25	186.1	103.88	89.43
V9	177.38	116.4	92.99	75.11	254.19	156.96	104.45	98.56
V10	112.84	106.77	84.49	68.62	237.72	155.55	115.81	90.25

5.3.2. Comprehensive benefits analysis. The multi-objective linear programming model constructed in this paper takes economic and ecological benefits as the objective function, and strives to achieve the maximum economic and ecological benefits after optimizing the distribution of native vegetation suitability in Hanzhong. In order to verify the validity of the model in this paper, five optimization models (denoted as M1, M2, M3, M4, M5, respectively) such as two-population genetic algorithm, weighted average method model, grey linear programming model, fuzzy linear programming model, and interval linear programming model were selected to calculate the comprehensive benefits of the optimization of the distribution of the habitability of the native vegetation in Hanzhong in the years of 2023, 2030, 2050 and 2080, and the results are shown in Table 7. As shown in Table 7, the unit of GDP in the table is billion yuan, and the unit of water demand (Water) is million cubic meters. The results show that this paper's model can realize the maximum benefits in all time periods. Specifically: in 2023, the economic benefits achieved by this paper's model in terms of GDP are 1.838 billion yuan, and the ecological benefits achieved in terms of water demand are 124,800 cubic meters. Compared with the M5 optimization model with the second best performance, this paper's model improves the economic and ecological benefits by 36.76% and 56.78%, respectively.In 2030, this paper's model improves the economic and ecological benefits by 72.21% and 136.39%, respectively, compared with the M5 model.The model M1, M^2, and M3 can no longer achieve the economic and ecological benefits of optimizing the distribution of the suitable distribution of the native vegetation after 2050. The optimization benefits of models M4 and M5 keep increasing, but the growth rate slows down obviously. However, the model in this paper not only can realize the continuous growth of the benefits of the optimization of the distribution of the habitability of native vegetation, but also the growth rate is increasing, and the benefit growth rate in 2050 compared with 2030 is 46.20% and 48.72%, and the benefit growth rate in 2080 compared with 2050 is 67.97% and 58.62%, respectively. It is fully demonstrated that the optimization model of this paper can maximize the economic and ecological benefits of the optimization of the distribution of native vegetation suitability in Hanzhong, and effectively achieve the predetermined objectives of the model. At the same time, the above results also show that the optimization of the distribution of native vegetation in Hanzhong can produce significant economic and ecological benefits, and with the passage of time, the amount of benefits will gradually increase, which is in line with the reality of the concept of ecological protection, and further illustrates the validity of this paper's model.

Table 7. Optimal allocation efficiency

Models	2023		2030		2050		2080	
	GDP	Water	GDP	Water	GDP	Water	GDP	Water
M1	2.86	0.89	3.07	1.74	3.07	1.74	3.07	1.74
M^2	4.83	3.21	5.04	5.68	5.04	5.68	5.04	5.68
M3	6.94	4.84	7.13	7.03	7.13	7.03	7.13	7.03
M4	10.72	6.79	11.22	10.96	7.42	11.94	7.69	12.03
M5	13.44	7.96	13.89	13.85	8.03	13.98	8.17	14.05
Ours	**18.38**	**12.48**	**23.92**	**32.74**	**34.97**	**48.69**	**58.74**	77.23

6. Conclusion

In this paper, a multi-objective linear programming model was constructed to optimize the distribution of native vegetation adaptability in Hanzhong City. In 2023, the optimized distribution areas of the 10 vegetation will be 281.64 km², 224.07 km², 252.78 km², 236.42 km², 284.39 km², 245.03 km², 201.31 km², 267.25 km², 254.19 km², and 237.72 km², respectively, which has a significant increase compared with that before optimization. In the prediction of 2080, the growth rates of the optimized adaptive distribution area of native vegetation in Hanzhong City were 49.61%, 35.51%, 36.41%, 28.11%, 15.36%, 24.75%, 27.92%, 28.40%, 31.22% and 31.52%, respectively. The results show that the multi-objective linear programming model in this paper can continuously optimize the growth and optimization of the distribution area of native vegetation in Hanzhong City. At the same time, compared with the other five optimization models, the proposed model can achieve the greatest economic and ecological benefits of optimizing the distribution of native vegetation adaptability.

Funding

Project 1: Study on Vegetation restoration of high and steep rock slope in Qinba Mountain Area (2021JQ-759).

Project 2: Holocene Paleoenvironmental evolution in Hanzhong Basin (SLGQD16-08).

Project 3: Research on the Mechanism and Path of Mountain Tourism Agriculture Boosting Rural Revitalization in Qinba Mountainous Area Based on Comprehensive Land Consolidation, supported by the Shaanxi Provincial Basic Research Program of Natural Science (2023-JC-QN-0310).

References

[1] de Alcântara Laudares, S. S., Borges, L. A. C., de Rezende, J. L. P., Bicalho, M. L., & de Barros, V. C. C. (2019). New Contours of the Native Vegetation Protection Law of 2012. Floresta e Ambiente, 26(4), e20160612.

[2] Fang, J. Y., Guo, K., Wang, G. H., Tang, Z. Y., XIE, Z. Q., Shen, Z. H., ... & Yu, D. (2020). Vegetation classification system and classification of vegetation types used for the compilation of vegetation of China. Chinese Journal of Plant Ecology, 44(2), 96.

[3] Chang, Y., Hou, K., Wu, Y., Li, X., & Zhang, J. (2019). A conceptual framework for establishing the index system of ecological environment evaluation-A case study of the upper Hanjiang River, China. Ecological Indicators, 107, 105568.

[4] Yan, Y., Liu, H., Bai, X., Zhang, W., Wang, S., Luo, J., & Cao, Y. (2022). Exploring and attributing change to fractional vegetation coverage in the middle and lower reaches of Hanjiang River Basin, China. Environmental Monitoring and Assessment, 195(1), 131-131.

[5] Kong, M., Li, Y., Zang, C., & Deng, J. (2023). The Impact Mechanism of Climate and Vegetation Changes on

the Blue and Green Water Flow in the Main Ecosystems of the Hanjiang River Basin, China. Remote Sensing, 15(17).

[6] Ren, H., Chen, C., Li, Y., Zhu, W., Zhang, L., Wang, L., & Zhu, L. (2023). Response of Vegetation Coverage to Climate Changes in the Qinling-Daba Mountains of China. Forests.

[7] Al-Dousari, A., Ramadan, A., Al-Qattan, A., Al-Ateeqi, S., Dashti, H., Ahmed, M., ... & Othman, A. (2020). Cost and effect of native vegetation change on aeolian sand, dust, microclimate and sustainable energy in Kuwait. Journal of Taibah University for Science, 14(1), 628-639.

[8] Chunni, L., Huang, Y., Wu, F., Liu, W., Yiqiu, N., Zhenrong, H., ... & Yu, L. (2021). Plant adaptability in karst regions. Journal of Plant Research, 134(5), 889-906.

[9] Zhu, H., & Tan, Y. (2022). Flora and Vegetation of Yunnan, Southwestern China: Diversity, Origin and Evolution. Diversity (14242818), 14(5).

[10] Anderson, K., Fawcett, D., Cugulliere, A., Benford, S., Jones, D., & Leng, R. (2020). Vegetation expansion in the subnival Hindu Kush Himalaya. Global Change Biology, 26(3), 1608.

[11] Ahrens, C. W., Andrew, M. E., Mazanec, R. A., Ruthrof, K. X., Challis, A., Hardy, G., ... & Rymer, P. D. (2020). Plant functional traits differ in adaptability and are predicted to be differentially affected by climate change. Ecology and Evolution, 10(1), 232.

[12] Deng, H., Yin, Y., & Han, X. (2020). Vulnerability of vegetation activities to drought in Central Asia. Environmental Research Letters, 15(8).

[13] Xu, H., Li, T. B., Chen, J. N., Liu, C. N., Zhou, X. H., & Xia, L. (2017). Characteristics and applications of ecological soil substrate for rocky slope vegetation in cold and high-altitude areas. Science of the Total Environment.

[14] Gavrilescu, M. (2021). Water, Soil, and Plants Interactions in a Threatened Environment. Water (20734441), 13(19).

[15] O'Loughlin, L. S., Panetta, F. D., & Gooden, B. (2021). Identifying thresholds in the impacts of an invasive groundcover on native vegetation. Scientific Reports, 11, 20512.

[16] Vignoni, A. P., Peralta, I. E., & Abraham, E. M. (2023). Fragmented areas due to agricultural activity: native vegetation dynamics at crop interface (Montecaseros, Mendoza, Argentina). Revista de la Facultad de Ciencias Agrarias UNCuyo, 55(2), 46-60.

[17] Yang, L., Xie, Z., Qin, Y., & Zheng, Z. (2019). Estimating Relations of Vegetation, Climate Change, and Human Activity: A Case Study in the 400 mm Annual Precipitation Fluctuation Zone, China. Remote Sensing, 11(10).

[18] Tashpulatov, Y. S., Kh, K. I., & Nurniyozov, A. A. (2019). Water and Coastal Water Vegetation of Various Types of Waters in The Samarkand Region. Bulletin of Pure and Applied Sciences Section A-Zoology, 38(2).

[19] Xie Linchen,Guo Ran,Yang Limin,Ozaki Yukihiro,Noda Isao,Xu Yizhuang & Huang Kun. (2023). A new approach to recognizing the correct pattern of cross-peaks from a noisy 2D asynchronous spectrum by detecting intrinsic symmetry via the Kolmogorov-Smirnov test. Physical chemistry chemical physics : PCCP(18),12863-12871.

[20] Yudun Li,Kuan Li,Rongqi Fan,Jiajia Chen & Yanlei Zhao. (2024). Multi-objective planning of distribution network based on distributionally robust model predictive control. Frontiers in Energy Research1478040-1478040.

[21] Prasantha Bharathi Dhandapani,Kalaiarasi Kalaichelvan,Víctor Leiva,Cecilia Castro & Soundaria Ramalingam. (2024). A Hybrid Fuzzy Mathematical Programming Approach for Manufacturing Inventory Models with Partial Trade Credit Policy and Reliability. Axioms(11),743-743.